

Outflow Boundary Condition Issues in Direct Numerical Simulation of Three-Dimensional Plane Wake Flow

M. J. Maghrebi¹, J. Soria²

Different choices of outflow boundary conditions are discussed in this paper and a proper choice is used in a hybrid numerical simulation which produces data to investigate the effect of outflow boundary condition. The convective outflow boundary condition with the wave speed as predicted from linear stability theory is used. The non-reflectiveness of this type is investigated and the reflection or the lack of reflection in a large deficit plane wake flow simulation is studied. The results of simulation reported in this paper indicate that the wave speed predicted from linear stability analysis is appropriate for the convective velocity at the outflow boundary of the large deficit plane wake flow. On the other hand the use of the freestream velocity for the convective speed at the outflow boundary of a large deficit plane wake flow also generates a serious feedback problem.

INTRODUCTION

The implementation of inflow and outflow conditions in simulations of free turbulent shear flows has been avoided by the use of "frozen turbulence approximation". In these types of simulations periodic boundary conditions are generally used in all spatial directions. Periodic boundary condition may be applied in a coordinate system moving with the mean flow. The physical problem which is nonhomogenous in the mean flow direction but homogenous in time is replaced by a computational problem that is homogenous in the main flow direction and nonhomogenous in the time domain. In other words, in these types of simulations, namely temporal simulations, the inflow conditions are replaced by initial conditions and the periodic boundary conditions are applied in the streamwise extent of the flow direction. On the other hand, in spatial simulations, it is necessary to specify boundary conditions particularly in the main flow direction. The specification of inflow and outflow boundary conditions plays a major difficulty in calculation of complex

engineering flows. Since flow at the outflow boundaries depends on the unknown flow outside the computational domain, an exact outflow boundary condition can not be implemented, but an approximation must be made. In the self similar region of plane wake flow, the application of periodic boundary conditions in the self similar coordinates is permitted. In more general cases, however, boundary conditions which are to be nonreflective in nature must be specified. In this work direct numerical simulation of three dimensional spatially-developing plane wake flow is performed to solve momentum and mass conservation equations.

The equations, which are known as Navier–Stokes equations and continuity equations, are solved for an incompressible medium. They are solved in a domain which is finite in the streamwise direction x , doubly infinite in the transverse direction y and homogeneous in the spanwise direction z . In the x direction, a family of compact finite difference schemes with spectral resolutions [7] and [11] is used. In y and z extents of the computational domain, a mapped spectral method [5] and a classical Fourier spectral method are used, respectively. The results of simulation are used to introduce a non-reflective boundary conditions at the outlet boundary of computational domain even for a large deficit plane wake flow. Dirichlet type for boundary conditions at the inflow and outflow bound-

1. Associate Professor, Dept. of Mech. Eng., Shahrood Univ. of Tech., Shahrood, Semnan, Iran, Email: javad@shahroodut.ac.ir.

2. Profesoor, Dept. of Mech. Eng., Monash Univ., Melbourne, Australia.

aries are imposed in the main stream direction. For this purpose, a family of finite difference scheme is used. Spatial simulation, which needs the specification of inflow and outflow boundary conditions, requires the use of a model at the outflow boundary of the computational domain. A poor choice of boundary condition at the outflow boundary can cause significant inaccuracies which can be deteriorated by the feedback effects in the simulation.

A buffer domain method, in conjunction with parabolization of the Navier Stokes equations, has been used to specify the outflow boundary condition by Bhaganagar et. al. [2]. This type of boundary condition smoothly reduces the disturbances to zero. Buffer domain technique is based on the idea that the disturbances are damped to zero at the vicinity of the outflow. Within the outlet region solutions were not physically valid, but the method prevents the reflection of the physical instabilities at the outflow boundary. They made validation of their results for both the linear and weakly nonlinear cases. They report that, for the steady Navier Stokes solution, the convective outflow boundary conditions returned good results. For non-steady problems, however, they did not yield good results, and as a result numerical instabilities developed. This was overcome by parabolising the Navier Stokes equations at the outflow boundaries. It was also reported that the proposed methods work well for elliptical problems. Artificial boundary conditions for simulation of inflow, outflow, and far-field problems were reviewed by Colonius [6]. This was studied for compressible turbulent shear flows. Inlet boundary conditions were set according to the linearization near the inlet boundary.

At the outflow boundary, however, the linearization of boundary conditions was not performed. Instead, absorbing layers and fringe methods adjacent to the exit boundary were proposed and employed. An extrapolation procedure for obtaining velocities at the outlet boundary in the simulation of incompressible flows around rigid bodies was studied by Nadeem et. al. [14] recently. The method is based on the radial variation of the velocity field (which can be estimated from mass conservation) at large distances from the rigid body. The numerical simulation involving specification of Neumann type boundary condition, however, requires the placement of the outflow boundary at a large distance in the downstream direction of the body.

The characteristics analysis was used to define non-reflecting outflow boundary conditions by Prosser [15]. The analysis was performed in terms of a low Mach number asymptotic series. The proposed boundary conditions, tested for three 2-dimensional inviscid flows and a two dimensional turbulent flow with a prescribed energy spectrum, allow the specification of non-reflecting outflow and inflow boundary conditions.

Since outflow boundary condition at the exit plane of a computational domain is not known, an approximation has been made. Different types of boundary condition are normally set at the outflow boundary of computational domain in spatially-developing simulation. The effects of different choices for outflow boundary conditions have been investigated by [4] and [13] in direct numerical simulation of spatially-developing flows. The outflow boundary conditions examined are free boundary condition, far field boundary condition, and convective outflow boundary condition. The last case is discussed in this paper by an emphasis on importance of convective velocity. The boundary conditions must be non-reflective to avoid feedback problems.

GOVERNING EQUATIONS

The governing equations for this study were derived from the full incompressible Navier-Stokes equations in rotational form [9]. Figure 1 shows the coordinate system and the computational domain in which the governing equations for the incompressible plane wake flow are solved. The inlet wake profile is specified by a base flow $U_0(y)$ that has a superimposed computational velocity. The wake flow is allowed to develop in the spatial direction x . A uniformly distributed entrainment velocity is specified for v at $\pm\infty$. Applying Newton's second law of motion for a Newtonian fluid particle gives the equations of motion. These equations, known as the Navier-Stokes equations, together with an equation representing mass conservation, are the governing equations for the incompressible plane wake flow. The governing equations (Equations (1) and (2)) have been nondimensionalized by the characteristic length ($b_{1/2}$)

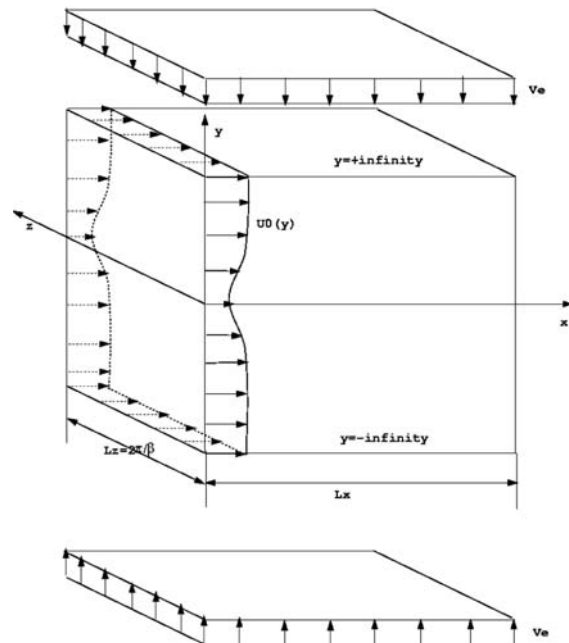


Figure 1. Coordinate system and computational domain.

and velocity scales (U_0).

$$\frac{\partial \mathbf{U}}{\partial t} = \mathbf{H} - \nabla(p + \frac{1}{2}\mathbf{U} \cdot \mathbf{U}) + \frac{1}{Re}\nabla^2\mathbf{U}, \quad (1)$$

$$\nabla \cdot \mathbf{U} = 0. \quad (2)$$

The vector $\mathbf{H} = (H_1, H_2, H_3) = \mathbf{U} \times \boldsymbol{\omega}$ contains the non-linear terms and $Re = U_0 b_{1/2} / \nu$. One of the main difficulties in solving the Navier–Stokes equations is the lack of information about the pressure at the boundaries. This is overcome by either using the staggered grid for the discretization, (which implies that different variables are evaluated at different grid points) or by eliminating the pressure term from the Navier–Stokes equation. The reduction of the number of independent variables and the disk space requirements are the advantage of the second method. Appropriate manipulation of the Navier–Stokes equations generate the following equations.

$$\frac{\partial \boldsymbol{\omega}}{\partial t} = \nabla \times \mathbf{H} + \frac{1}{Re}\nabla^2\boldsymbol{\omega}, \quad (3)$$

$$\frac{\partial \nabla^2 \mathbf{U}}{\partial t} = \nabla \times (\nabla \times \mathbf{H}) + \frac{1}{Re}\nabla^4 \mathbf{U}. \quad (4)$$

Equations (3) and (4) are the evolution equations responsible for the time-advancement in the simulation. Detailed discussion is given in [9]. The instantaneous velocity, $\mathbf{U} = (U, V, W)$, is decomposed into the base flow ($U_0(y), 0, 0$), the entrainment velocities, ($U_e(y), V_e(y)$) and the computational variables ($u(x, y, z, t)$, $v(x, y, z, t)$, $w(x, y, z, t)$) as indicated by Equations (5), (6) and (7).

$$U(x, y, z, t) = u(x, y, z, t) + U_0(y) + xU_e(y) \quad (5)$$

$$V(x, y, z, t) = v(x, y, z, t) + V_e(y) \quad (6)$$

$$W(x, y, z, t) = w(x, y, z, t) \quad (7)$$

V_e is a smooth and continuous function in y , which tends to the entrainment velocity. It is independent of x , t and z . $U_e(y)$ and $V_e(y)$ are related such that they solely satisfy the mass conservation for the entrainment velocity component. (e.g. $U_e(y) = -\partial V_e(y) / \partial y$.) The entrainment velocities are introduced to take an account for incorporation of non-turbulent region (freestream) into the turbulent region (wake center) or the diffusion of the wake flow into the ambient (freestream). The decomposition is performed to preserve zero value for the velocity components at the freestream boundaries.

Use of the streamwise components of Equations (3), (4) and the decomposition shown by Equation (5) yields:

$$\frac{\partial}{\partial t}\nabla^2 u = \nabla_{\perp}^2 H_1 - \frac{\partial^2}{\partial x \partial y} H_2 - \frac{\partial^2}{\partial x \partial z} H_3 + \frac{1}{Re}\nabla^4 U, \quad (8)$$

and

$$\frac{\partial}{\partial t}\omega_1 = \frac{\partial}{\partial y} H_3 - \frac{\partial}{\partial z} H_2 + \frac{1}{Re}\nabla^2 \omega_1, \quad (9)$$

where

$$\nabla_{\perp}^2 \equiv \frac{\partial^2}{\partial y^2} + \frac{\partial^2}{\partial z^2}. \quad (10)$$

As indicated by Maghrebi [9] the choice of streamwise components in Equation (9) is preferred because only ω_1 is the vorticity component with a known boundary condition. It can be directly recovered from its definition ($\omega_1 = \partial w / \partial y - \partial v / \partial z$). Equations (8), (9) and the convective outflow boundary condition are responsible for the time-advancement of the simulation. With the help of the continuity equation and the definition of ω_1 , the spanwise velocity can be obtained

$$\nabla_{\perp}^2 w = \frac{\partial \omega_1}{\partial y} - \frac{\partial^2 u}{\partial x \partial z}. \quad (11)$$

The cross-stream velocity component v is recovered directly from the continuity equation

$$\frac{\partial v}{\partial y} = -\frac{\partial u}{\partial x} - \frac{\partial w}{\partial z}. \quad (12)$$

The other vorticity components are calculated using their definitions. Since the governing equations are directly solved without the use of any modeling, the solution method is called *direct* numerical simulation (DNS).

BOUNDARY CONDITIONS

The boundary conditions discussed here are related to the computational variables rather than the velocity components. Equation (8) is a fourth-order, partial differential equation, so it requires four boundary conditions. The u velocity is specified at the inlet ($x = 0$) and the outlet boundaries ($x = L_x$). With the help of the continuity equation $\partial u / \partial x$ is also determined at the inflow and outflow boundaries

$$\frac{\partial u}{\partial x} = -\frac{\partial v}{\partial y} - \frac{\partial w}{\partial z}. \quad (13)$$

The former and the latter are known as Dirichlet and Neumann type boundary conditions, respectively. The boundary conditions are set to zero in the transverse direction. Since the wake flow is assumed to be

homogeneous in the z direction, periodic boundary conditions are used over the domain $0 \leq z \leq L_z$. Equation (9) is second order and is supplemented by the Dirichlet boundary condition at the ending boundaries. It is specified according to the definition of ω_1 :

$$\omega_1 = \frac{\partial w}{\partial y} - \frac{\partial v}{\partial z}. \quad (14)$$

In the numerical simulations, the instantaneous velocity component at the inlet boundary is specified using a Gaussian velocity profile which is superimposed by some perturbations. The perturbations are introduced in the form of a traveling wave. The Gaussian profile which corresponds to the experimental investigation of Sato & Kuriki [16] is chosen $U(y) = 1 - 0.692 \exp(-\ln(2)y^2)$. The perturbation part, which consists of a combination of linear eigenfunctions obtained from the linear stability calculations, is specified for the inflow boundary condition. In other words,

$$\begin{aligned} \mathbf{u} = & \text{Real}[A_{2DF} \hat{\mathbf{u}}_{2DF}(y) \exp(-i\omega t) \\ & + A_{2DS} \hat{\mathbf{u}}_{2DS}(y) \exp(-i\omega t/2) \\ & + A_{2DSS} \hat{\mathbf{u}}_{2DSS}(y) \exp(-i\omega t/4) \\ & + A_{3D} \hat{\mathbf{u}}_{3D}(y) (\exp(\frac{\beta z - i\omega t}{2}) + (\exp(\frac{-\beta z - i\omega t}{2})))]]. \end{aligned} \quad (15)$$

where

- $\hat{\mathbf{u}}_{2DF}(y)$, $\hat{\mathbf{u}}_{2DS}(y)$ and $\hat{\mathbf{u}}_{2DSS}(y)$ are the velocity eigenfunctions corresponding to the most amplified eigenmodes of the two-dimensional Orr–Sommerfeld equation. $\hat{\mathbf{u}}_{2DF}(y)$, $\hat{\mathbf{u}}_{2DS}(y)$ and $\hat{\mathbf{u}}_{2DSS}(y)$ are obtained at the frequency of fundamental, subharmonic and second subharmonic forcings (ω , $\omega/2$ and $\omega/4$, where $\omega = 0.614$).
- $\hat{\mathbf{u}}_{3D}(y)$ contains the velocity eigenfunctions corresponding to the maximum growth rate of the Orr–Sommerfeld equation for three-dimensional disturbances. The maximum growth rate occurs at $\omega = 0.307$ ([10]).
- A_{2DF} , A_{2DS} and A_{2DSS} are the amplitude of two-dimensional forcings which correspond to fundamental, subharmonic and second subharmonic frequencies.
- A_{3D} is the amplitude of three-dimensional forcing.
- β is the spanwise wavenumber of the subharmonic or second subharmonic mode.

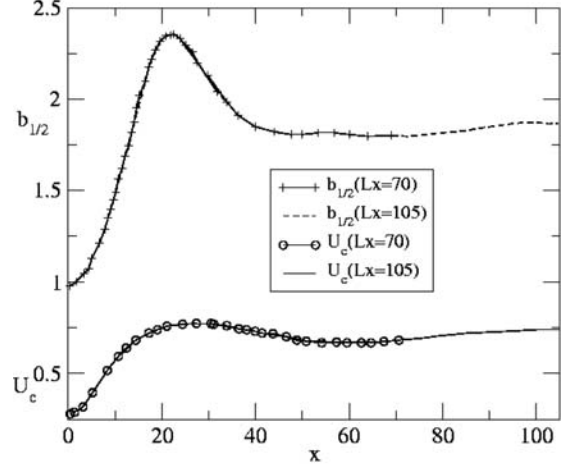


Figure 2. Spatial development of mean centerline velocity and wake halfwidth using two sets of results from two-dimensional simulations with identical parameters except L_x and N_x which are 1.5 times larger than those used in simulation with the smaller domain.

OUTFLOW BOUNDARY CONDITIONS

The accuracy of different types of outflow boundary conditions in a two-dimensional, spatially-developing mixing layer has been investigated by Miyauchi *et al.* [13]. They conclude that the free outflow boundary condition ($\partial u_i / \partial t = 0$) is not appropriate for the spatially-developing flow problems. They tested four other kinds of the outflow boundary conditions

- an inviscid convective boundary condition using mean velocity profile ($\partial u_i / \partial t + U \partial u_i / \partial x = 0$),
- an inviscid convective boundary condition using the local velocity ($\partial u_i / \partial t + u_j \partial u_i / \partial x = 0$),
- a viscous mean velocity convective boundary condition ($\partial u_i / \partial t + U \partial u_i / \partial x - \frac{1}{Re} (\partial^2 u_i / \partial x_j^2) = 0$),
- a viscous local velocity convective boundary condition ($\partial u_i / \partial t + u_j \partial u_i / \partial x - \frac{1}{Re} (\partial^2 u_i / \partial x_j^2) = 0$).

The viscous convective outflow boundary condition with local velocity was found to be inconsistent with the solution of the Navier–Stokes equations as it suggests zero pressure gradients. The inviscid convective outflow boundary condition (with local velocity as convection speed) is also reported to be inaccurate. The accuracy of the viscous convective boundary condition (with mean velocity as convection speed) is better than that of the inviscid case. The accuracy was found more pronounced at lower Reynolds number. In this study, the inviscid convective boundary condition $\partial u_i / \partial t + c \partial u_i / \partial x = 0$ is used to generate the Dirichlet outflow boundary conditions. The accuracy of the solution in the simulation using small computational domain is sensitive to the choice of the convective velocity. It has been shown by Maekawa *et al.* [8] that the choice of freestream velocity is appropriate for the simulation

of the far wake. However, the use of the free-stream velocity as the convective speed at the outflow boundary of the simulation with small computational domain is not appropriate. This generates significant inaccuracies in the solutions. In this work, the convective velocity is set as the wave speed according to the linear stability calculation. That is

$$\begin{aligned} v_{wave} &= \lambda_x/T \\ &= (2\pi/\alpha_r)/(2\pi/\omega) \\ &= \omega/\alpha_r. \end{aligned}$$

which represents the wave speed in the streamwise direction of a spatially evolving flow. Here, ω and α_r are the circular frequency and the wavelength in streamwise direction, respectively. Detailed discussions are given in [10].

INITIAL CONDITIONS

An unforced, two-dimensional wake flow simulation whose inlet boundary contains a base profile (Gaussian mean velocity distribution) provides the initial conditions for the forced wake simulations. A uniformly distributed Gaussian mean velocity profile at all x stations is the initial condition for the unforced two-dimensional wake simulation. Hence, the initial condition for ω_1 is zero³ for any of the numerical simulations conducted. Prior to any statistical analysis, it is ensured that the initial conditions for each simulation have been washed out from the computational domain. In other words, any particle at the inlet (at $x = 0$) must be allowed to leave the outlet boundaries (at $x = L_x$). The wake flow must also reach the statistically stationary state in which the mean velocity component is independent of time.

RESULTS AND DISCUSSIONS

The proposed algorithm was successfully applied to many three and two dimensional cases. The only difference between these simulations correspond to the inlet forcings. In other words the inflow boundary conditions for each case study are different. Among all of the simulations conducted, four are three dimensional. For detailed information regarding each case study refer to Maghrebi [9]. In the current work two cases of 2-D simulations are studied. These are discussed to investigate the sensitivity of the flow to the convective boundary condition (using $c = 0.86$ as the wavespeed obtained from linear stability calculations). Both simulations have the same parameters except that the simulation with a larger domain used a length (L_x) and grid numbers (N_x) of one and a half times larger than those used in the simulation with smaller

domain. The spatial increment (Δx) is the same for both cases. The parameters used in the simulation with a smaller domain are: $N_x = 240$, $N_y = 96$, $N_z = 2$, $\beta = 6$, $Re = 500$, $U(y) = 1 - 0.692 \exp(-\ln(2)y^2)$ and $c = 0.86$. A frequency of $\omega = 0.614$, which corresponds to the maximum growth rate of the most amplified eigenvalues is used. The numerical results of both simulations for the mean centerline velocity and the wake halfwidth are shown in Figure 2. The results indicate that the mean characteristics for both of the simulations are identical. This means that the choice of the convective velocity ($c = 0.86$) is appropriate for the near wake simulation.

In other words convective outflow boundary conditions using c as predicted from linear stability analysis is non-reflective type.

$$\frac{\partial \psi}{\partial t} = -c \frac{\partial \psi}{\partial x} \quad (16)$$

where ψ is replaced by each of the velocity components. These boundary conditions with ψ replaced by each of the velocity components are used to generate the Dirichlet boundary conditions for the spatially-developing plane wake flow simulation. The freestream velocity is found to be an appropriate one for c in the simulation of small and moderate deficit wakes [8]. Therefore, the use of wave speed predicted from linear stability theory is appropriate for the convective velocity at the outflow boundary of the large deficit plane wake simulation. The use of the freestream velocity for the convective speed at the outflow boundary of a large deficit plane wake flow generates a serious feedback problem. The vorticity contours of these two simulations are shown in Figure 3. Although both contours

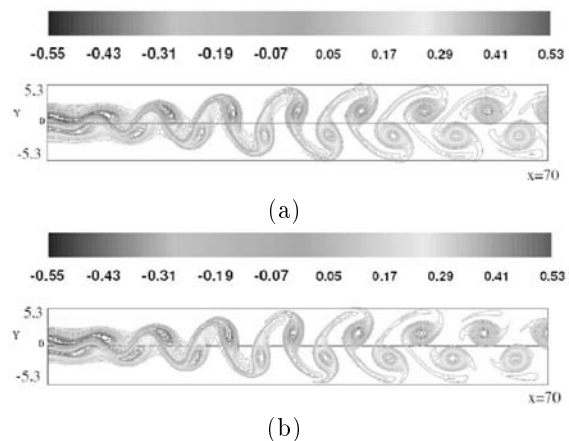


Figure 3. Vorticity contours of two-dimensional simulation using L_x in (a) and $1.5L_x$ in (b) as computational length (Parameters for simulation with smaller domain are: $N_x = 240$, $N_y = 96$, $N_z = 2$, $\beta = 6$, $Re = 500$, $U(y) = 1 - 0.692 \exp(-\ln(2)y^2)$, $c = 0.9$, $L_x = 70$, $\omega = 0.614$ and $t = 500$). Maximum and minimum value of contours are 0.540533, -0.546965 in (a) and 0.528796, -0.549807 in (b), respectively.

3. This is because any two-dimensional solution only contains spanwise component for the vorticity.

indicate that the wake flows are similar and smoothly convected downstream, there is a small change in the maximum of the contour levels. The difference means that even if a proper choice for the convective velocity is used, we should avoid collecting the data at the vicinity of the outlet boundary. This can be related to the fact that in the far wake regions where the mean characteristics of the wake are approximately constant, the wavelength is larger than that of appearing in the near wake. Hence, the local wave speed at the outflow boundary of the near wake is smaller than that of the far wake. Moreover, the wave speed predicted from the linear stability theory, which is quite valid for the linear region of the wake development, suggests the convective speed of 0.86 for the case which uses the frequency of 0.614 as a source for perturbation of the inflow boundary. If the computational domain is small, then the convective velocity is better approximated by the wave speed. Since the length of the computational domain is neither large (to obtain a small deficit wake at the outflow boundary) nor small (to have the outflow boundary in the linear region), a number between 0.86 (corresponding to the wave speed in the linear region of the wake) and one (corresponding to the small deficit wake where the free-stream velocity is used for the convective velocity) may also be used with care.

CONCLUSION

Direct numerical simulation of three dimensional spatially-developing plane wake flow is used to solve the governing equation of an incompressible plane wake flow. These equations are solved in a domain which is finite in the streamwise, doubly infinite in the cross-stream direction and periodic in the spanwise direction. In the streamwise direction a family of Pade finite difference scheme of Lele [7] and Mahesh [11] is used. In the cross-stream and spanwise directions, a mapped spectral method of Cain *et. al.* [5] and a Fourier spectral techniques are used, respectively. Different choices of outflow boundary conditions are discussed in this paper and a proper choice is used in a hybrid numerical simulation which produces data to investigate the effect of outflow boundary condition. The convective outflow boundary condition with the wave speed as predicted from linear stability theory is used. This type is found to be non-reflective and free from reflective problems even in a large deficit plane wake flow simulation. The contourplot of vorticity and the evolution of wake halfwidth and the wake centerline for both simulations indicates that the choice is quite appropriate for large deficit spatially-developing plane wake flow simulation. The results of two distinct simulations are used to assess the validity of a non-reflective boundary condition at the outlet boundary of computational domain. The results are valid for a large

deficit plane wake flow indicating less computational efforts are required for spatially-developing plane wake flow. The results of simulation reported in this paper indicate that the wave speed predicted from linear stability analysis is appropriate for the convective velocity at the outflow boundary of the large deficit plane wake flow. On the other hand, the use of the freestream velocity for the convective speed at the outflow boundary of a large deficit plane wake flow also generates a serious feedback problem.

REFERENCES

1. Betchov R., Criminale W. O., *Stability of Parallel Flow*, New York, Academic Press, (1967).
2. Bhaganagar K., Rempfer D. and Lumley J., "Direct Numerical Simulation of Spatial Transition to Turbulence Using Fourth-Order Vertical Velocity Second-Order Vertical Vorticity Formulation", *Journal of Computational Physics*, **180**, (2002).
3. Buell J. C., "A Hybrid Numerical Method for Three-Dimensional Spatially-Developing Free-Shear Flows", *J. Comp. Phys.*, **95**, PP 313-338(1991).
4. Buell J. C. and Huerre P., "Inflow and Outflow Boundary Conditions and Global Dynamics of Spatial Mixing Layers", *N89-24540*, Proceedings of the Summer Program, PP 19-27(1988).
5. Cain A. B., Ferziger J. H. and Reynolds W. C., "Discrete Orthogonal Function Expansions for Non-uniform Grids Using the Fast Fourier Transform", *J. Comp. Phys.*, **56**, PP 272-286(1984).
6. Colonus T., "Modeling Artificial Boundary Conditions for Compressible Flow", *Annu. Rev. Fluid Mech.*, (2004).
7. Lele S. K., "Compact Finite Difference Schemes with Spectral-Like Resolution", *J. Comp. Phys.*, **103**, PP 16-42(1992).
8. Maekawa H. and Mansour N. N., "Direct Numerical Simulations of a Spatially-Developing Plane Wake", *JSME International Journal*, **35**(4), PP 543-548(1992).
9. Maghrebi M. J., "A Study of the Evolution of Intense Focal Structures in Spatially-Developing Three-Dimensional Plane Wakes", Ph.D. Thesis, Department of Mechanical Engineering, Monash University, Clayton, Victoria, Australia(1999).
10. Maghrebi M. J., "Orr Sommerfeld Solver Using Mapped Finite Difference Scheme for Plane Wake Flow", *Journal of Aerospace Science and Technology*, *JAST*, **2**(2), PP 55-63(2005).
11. Mahesh K., "A Family of High-Order Finite Difference Schemes with Good Spectral Resolution", *J. Comp. Phys.*, **145**, PP 332-358(1998).
12. Meiburg E. and Lasheras J. C., "Comparison Between Experiments and Numerical Simulations of Three-Dimensional Plane Wakes", *Phys. Fluids*, **30**(3), PP 623-625(1987).

13. Miyauchi T., Tanahashi M. and Suzuki M., "Inflow and Outflow Boundary Conditions for Direct Numerical Simulations", *JSMÉ International Journal*, **39**(2), PP 305-314(1996).
14. Hasan N., Anwer S. F. and Sanghi S., "On the Outflow Boundary Condition for External Incompressible Flows: A New Approach", *Journal of Computational Physics*, **206**, (2005).
15. Prosser R., "Improved Boundary Conditions for the Direct Numerical Simulation of Turbulent Subsonic Flows", *Journal of Computational Physics*, **207**, (2005).
16. Sato H. and Onda Y., "Detailed Measurements in the Transition Region of a Two-Dimensional Wake", *Report No. 453*, Institute of Space and Aeronautical Science, University of Tokyo, PP 317-377(1970).